Dissection of the Functional Role of Structural Elements of Tyrosine-63 in the Catalytic Action of Human Lysozyme†

Michiro Muraki,*,‡ Kazuaki Harata,§ and Yoshifumi Jigami‡

Biological Chemistry Division, National Chemical Laboratory for Industry, Tsukuba, Ibaraki 305, Japan, and Bioengineering Department, Research Institute for Polymers and Textiles, Tsukuba, Ibaraki 305, Japan

Received April 15, 1992

ABSTRACT: The functional role of tyrosine-63 in the catalytic action of human lysozyme (EC 3.2.1.17) has been probed by site-directed mutagenesis. In order to identify the role of Tyr63 in the interaction with substrate, both the three-dimensional structures and the enzymatic functions of the mutants, in which Tyr63 was converted to phenylalanine, tryptophan, leucine, or alanine, have been characterized in comparison with those of the wild-type enzyme. X-ray crystallographical analysis of the mutant enzyme at not less than 1.77-Å resolution indicated no remarkable change in tertiary structure except the side chain of 63rd residue. The conversion of Tyr63 to Phe or Trp did not change the enzymatic properties against the noncharged substrate (or substrate analogs) largely, while the conversion to Leu or Ala markedly reduced the catalytic activity to a few percent of wild-type enzyme. Kinetic analysis using *p*-nitrophenyl penta-*N*-acetyl-β-(1→4)-chitopentaoside (PNP-(GlcNAc)$_5$) as a substrate revealed that the reduction of activity should mainly be attributed to the reduction of affinity between enzyme and substrate. The apparent contribution of the phenolic hydroxyl group and the phenol group in the side chain of Tyr63 was estimated to 0.4 ± 0.4 and 2.5 ± 0.8 kcal mol^{-1}, respectively. The result suggested that the direct contact between the planar side-chain group of Tyr63 and the sugar residue at subsite B is a major determinant of binding specificity toward a electrostatically neutral substrate in the catalytic action of human lysozyme.

Recognition of a carbohydrate by proteins serves essential roles in many important biological functions including the defense action against microorganisms, the uptake of sugars into cells, and so on (Quiocho, 1986). Human lysozyme is a hydrolytic enzyme that recognizes either β-(1→4)-linked homopolymer of *N*-acetylglucosamine (chitin) or β-(1→4)-linked alternative copolymer composed of *N*-acetylglucosamine and *N*-acetylmuramic acid (bacterial cell wall polysaccharide) as its substrates. Human lysozyme is one of the most structurally well-characterized carbohydrate binding proteins. The tertiary structures of both the uncomplexed state (Artymiuk & Blake, 1981) and the complex state with either *N*-acetylglucosamine trisaccharide (Matsushima et al., 1990) or pentasaccharide (Inaka et al., 1990) have been determined by high-resolution X-ray crystallographic studies. Recently, the structure in solution also has been investigated using two-dimensional ^{1}H-NMR (Redfield & Dobson, 1990) and ^{15}N-NMR (Ohkubo et al., 1991). Among the tryptophan residues in the active cleft of a homologous enzyme, hen egg-white lysozyme, Trp62 has been extensively modified using chemical modifications (Hayashi et al., 1965; Kuroda et al., 1975; Yamasaki et al., 1976) and site-directed mutagenesis (Kumagai & Miura, 1989), and the modified enzymes have been characterized both functionally (Imoto et al., 1974; Shrake & Rupley, 1980) and structurally (Blake et al., 1981). In some mammalian lysozymes, including human lysozyme, this tryptophan residue is replaced with a tyrosine residue. The effect of this replacement on the physicochemical properties and the enzymatic properties has been interesting from the viewpoint of comparative biochemistry (Imoto et al., 1972; Osserman et al., 1972). Nevertheless, the information on the functional role of the corresponding residue, Tyr63, in human lysozyme is limited partly due to the lack of the chemical modification method specific to this residue. Our previous study (Muraki et al., 1987) revealed that the existence of an aromatic residue at position 63 is responsible for the effective hydrolysis of glycol chitin, but not for the lysis of the bacterial substrate by the enzymatic characterization of the mutants in which Tyr63 is converted to Phe, Trp, or Leu. However, no direct evidence about the structural change caused by the mutations has been obtained, and the substrate used for kinetic analysis was confined to bacterial cells, which is not chemically uniform and is highly negatively charged under the assay conditions. These defective points in characterization have left the interpretation of the experimental results concerning the functional role of Tyr63 in the recognition of the sugar residue still ambiguous. In the present study, in order to further clarify this point and to dissect the functional role of structural elements of tyrosine-63 in the catalytic action of human lysozyme, we determined the detailed structures of mutant enzymes including a newly synthesized mutant, in which Tyr63 was converted to Ala, by X-ray crystallography and characterized their enzymatic properties using mainly a chemically uniform substrate, *p*-nitrophenyl penta-*N*-acetyl-β-(1→4)-chitopentaoside (PNP-(GlcNAc)$_5$)[1] in comparison with wild-type enzyme.

MATERIALS AND METHODS

Materials. Authentic human lysozyme was purchased from Green Cross Co., Japan, and further purified by using a cation-

† This work was supported by a grant from the Science and Technology Agency Japan.

* To whom correspondence should be addressed.

‡ National Chemical Laboratory for Industry.

§ Research Institute for Polymers and Textiles.

[1] Abbreviations: (GlcNAc)$_2$, β-1,4-linked dimer of *N*-acetyl-D-glucosamine; (GlcNAc)$_3$, β-1,4-linked trimer of *N*-acetyl-D-glucosamine; PNP-(GlcNAc)$_5$, *p*-nitrophenyl β-1,4-linked pentamer of *N*-acetyl-D-glucosamine; PNP-(GlcNAc)$_n$, *p*-nitrophenyl β-1,4-linked *n*-mer of *N*-acetyl-D-glucosamine; HPLC, high-pressure liquid chromatography; rms, root mean square.

0006-2960/92/0431-9212$03.00/0

Table I: Some Crystallographic Properties of Wild-Type and Mutant Human Lysozymes

	wild type[a]	Y63F	Y63W	Y63L	Y63A
space group	$P2_12_12_1$	$P2_12_12_1$	$P2_12_12_1$	$P2_12_12_1$	$P2_12_12_1$
lattice constants					
a (Å)	57.13	57.19	57.15	57.19	57.14
b (Å)	60.99	60.98	61.05	60.90	61.04
c (Å)	32.89	33.02	33.02	33.01	32.99
unique reflections[c]		10792	11066	7608	10700
resolution (Å)	1.5	1.70	1.70	1.77	1.70
r_{merge} (%)					
1st crystal		9.0	9.0	8.5	9.3
2nd crystal		10.1	8.9	8.6	8.5
R-factor[b]	0.187	0.182	0.181	0.182	0.186
Δ_{bond} (Å)		0.013	0.013	0.013	0.013
Δ_{angle} (deg)		2.7	2.7	2.9	2.7
av temp factor of side chain atoms of					
63th residue	51.74	29.78	25.26	27.93	13.91
Trp64	16.25	11.12	11.35	10.69	11.21

[a] Data from the Brookhaven Protein Data Bank (Artymiuk & Blake, 1984; data set name, 1LZ1). [b] R-factor = $\Sigma||F_o| - |F_c||/\Sigma|F_o|$. [c] After the merge of two data sets. Δ_{bond} and Δ_{angle} are the root mean square deviations of bond length and angles from ideal stereochemistry.

exchange column (MonoS HR5/5, Pharmacia) as described previously (Jigami et al., 1986). The concentration was determined on the basis of the absorption coefficient ($A^{1\%}_{280nm}$ = 25.65 cm^{-1}) (Parry et al., 1969). Lyophilized *Micrococcus luteus* cells were from Sigma. PNP-$(GlcNAc)_n$ (n = 1–5) (more than 97% purity), $(GlcNAc)_2$ (more than 99%), and $(GlcNAc)_3$ (more than 99%) were obtained from Seikagaku Co., Japan. All other chemical reagents were of biochemical or analytical grade.

A mutant gene coding Ala63 human lysozyme was constructed as described previously (Muraki et al., 1989). An oligonucleotide primer used for the mutagenesis was ATTAACTCTAGAGCCTGGTGT. Themismatchisshown by underlining in the primer sequence.

Crystallization and Structural Determination of Mutant Human Lysozymes. All procedures concerning the production and the purification of mutant human lysozymes were the same as reported previously (Jigami et al., 1986). The secretion level of the Ala63 mutant was somewhat higher (1.5–2 times) than other mutants. The concentration of purified mutant protein was determined by the dye-binding method using a protein concentration assay kit (Bio-Rad). Authentic human lysozyme was used as the standard.

Crystallization of all mutant enzymes was carried out as described previously (Muraki et al., 1991) using the repeated seeding procedure (Thaller et al., 1985). Typically, well-shaped prisms of 0.5 mm × 0.5 mm × 1.0 mm were obtained. All the crystals of mutant human lysozymes concerning Tyr63 were isomorphous with the orthorhombic crystal of the wild-type enzyme (Osserman et al., 1969). Diffraction data were collected on an Enraf-Nonius FAST diffractometer with a GX21 generator (40 kV, 60 mA, and focal spot size of 0.3 × 3 mm). For each mutant, two independent crystals were employed for data collection. Crystallographic refinement was carried out using a software package, X-PLOR (Brünger et al., 1987). A set of protein coordinates of the wild-type human lysozyme (Protein Data Bank, entry code 1LZ1) in which Tyr63 was replaced with the corresponding residue depending on each mutation was used as an initial model for the structure determination. Some crystallographic properties of wild-type and mutant human lysozymes are summarized in Table I. The coordinate errors were estimated to be about 0.2 Å for all mutants according to Luzzati (1952). The coordinates have been deposited with the Protein Data Bank, Brookhaven National Laboratory, Upton, Long Island, NY.

Geometrical Analysis of Mutant Human Lysozymes. The geometrical analysis and the calculation of accessible surface area (Lee & Richards, 1971) were performed using X-PLOR. The probe radius used for the calculation of accessible surface area is 1.4 Å.

Measurement of CD Spectra. CD spectra were measured with a JASCO J-600 spectropolarimeter at 25 °C. The proteins were dissolved in 25 mM sodium phosphate buffer (pH 8.0) plus 0.27 M NaCl, and the concentrations were adjusted to 0.33 mg/mL. The data are expressed in terms of mean residue ellipticity.

Fluorometric Methods. Fluorometric measurements were performed with a Kontron SFM25 spectrofluorimeter at 30 °C in MacIlvaine's buffer (pH 7.2) (McIlvaine, 1921) composed of 100 mM citric acid and 50 mM disodium hydrogen phosphate. The excitation wavelength was 285 nm. The concentration of protein was adjusted to 3.0 μM. Dissociation constants with $(GlcNAc)_3$ were estimated by fluorometric titration according to the method of Chipman et al. (1967) by plotting log $[(F_0 - F)/(F - F_\infty)]$ against log [s], where F_0, F, F_∞ are the relative fluorescence intensity of human lysozyme alone, that of human lysozyme in the presence of a concentration [s] of $(GlcNAc)_3$, and that of human lysozyme saturated with $(GlcNAc)_3$, respectively.

Assay of Enzymatic Activity. (1) Against M. luteus Cells. The activity against *M. luteus* cells was determined spectrophotometrically basically according to the turbidometric method (Locquet et al., 1968). For the comparison of lysis curves, the lysis of *M. luteus* cells in 50 mM potassium phosphate buffer (pH 6.2) was monitored. Measurements were carried out at 25 °C in a thermostated cell with a Shimadzu UV-160 recording spectrophotometer.

(2) Against PNP-$(GlcNAc)_5$. The action profiles against PNP-$(GlcNAc)_5$ and the initial velocity of hydrolysis of PNP-$(GlcNAc)_5$ were determined by monitoring the elution pattern of the reaction mixture on HPLC column. Chromatography was performed with an Asahipack NH_2P-50 column (4.6 × 250 mm) in a Shimadzu LC-6A liquid chromatography equipped with a SPD-6AV spectrophotometer. The flow rate was 1.0 mL/min with acetonitrile/water (88/12) eluent. The elution pattern was monitored by measuring ultraviolet absorbance at 300 nm due to the *p*-nitrophenyl group. The peak areas of both the initial substrate and the reaction products were measured with a Shimadzu CR3-A integrator and were converted into a molar concentration using the standard curves obtained with authentic samples of PNP-$(GlcNAc)n$ (n = 1–5). The substrate concentrations of 3.0 × 10^{-4}–3.0 × 10^{-5} M and the enzyme amounts of 2–20 μg (for wild-type, Y63F, and Y63W mutants) and 50–90 μg (for

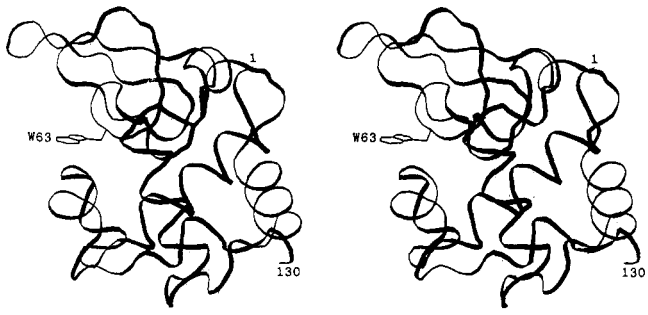

FIGURE 1: Backbone structure of the Y63W human lysozyme. The side chain of the Trp63 residue is shown by thin lines.

Y63L and Y63A mutants) were used. Reaction was performed at 37 °C in a final volume of 1.8 mL of 100 mM sodium citrate buffer (pH 5.0), and samples for HPLC assay (20 μL) were taken at intervals during the incubation. For the estimation of initial velocity, the extent of reaction was set not to exceed ca. 15% in order to ensure the linearity of the hydrolysis of PNP-$(GlcNAc)_5$.

RESULTS

Structures of Mutant Human Lysozymes. The tertiary structures of all mutants in this study were very similar to the structure of the wild-type human lysozyme (Artymiuk & Blake, 1981). As an example, the backbone structure of the Y63W mutant is shown in Figure 1. The 63rd residue is located at the end of the loop region which is connected to the anti-parallel β-sheet including the 58–61th strand. The side-chain group is exposed to solvent in the active-site cleft. In Figure 2, $(F_o - F_c)$ electron density maps of each mutant in the vicinity of the 63rd residue were shown. The well-shaped and strong electron densities in the map confirmed the 63rd residue of corresponding mutations. However, for the residues Phe63, Trp63, or Leu63, the electron density of the side chain in $(2F_o - F_c)$ electron density maps was weaker than the adjacent residue, Trp64, and the final temperature factor of the side chain was larger than that of Trp64 (Table I). This suggests that the conformations of the side chain of the 63rd residue in these mutants are fairly flexible as is the case in wild-type human lysozyme, but the disorder found in the X-ray analysis of wild-type enzyme at 1.5-Å resolution (Phillips et al., 1987) is not observed in this study.

In Figure 3, the superimposed structures of the wild-type and of each mutant human lysozyme are shown. In the Y63F mutant, the phenyl group of Phe63 is in the same orientation as the phenol group of Tyr63 in the wild-type enzyme. The benzene ring is found to be almost overlapped in both structures with the rms difference of 0.03 Å for six corresponding carbon atoms (Figure 3a). The indole group of Trp63 in the Y63W mutant shares the same plane with the phenol group of the wild-type enzyme. The tortion angle of the C^α–C^β bond is not affected in spite of the bulkier side-chain group (Figure 3b). The nonpolar side chain of Leu63 in the Y63L mutant is also found to be in a similar orientation with the side cain of Tyr63 in the wild-type enzyme. However, the C^β–C^γ bond is so rotated that one methyl group is positioned on the plane through the phenol group of Tyr63 in the wild-type enzyme (Figure 3c). The methyl group of Ala63 in the Y63A mutant is located at almost the same position as the C^β atom of Tyr63 in wild-type enzyme (Figure 3d). The rms differences between corresponding atomic positions in wild-type and mutant human lysozymes are summarized in Table II for all the main-chain atoms, the side-chain atoms of the major residues composing the active site (Glu35, Asp53, Trp64, Asp102, and Trp109), and the side-chain atoms of the catalytic residues (Glu35 and Asp53), respectively. None of these values are more than the estimated coordinate error (ca. 0.2 Å) indicating that the replacements of the 63rd residue in this study did not significantly affect either the backbone structure or the active-site structure of the human lysozyme.

CD spectra in the near-ultraviolet (245–310 nm) were compared among wild type, the mutants, and hen egg-white lysozyme (Figure 4). The shapes of spectra were essentially identical among wild type and all mutants, suggesting the conformational similarity of these molecules in solution. One of the structural features that is absent in human lysozyme but present in hen egg-white lysozyme is the adjacent pair of tryptophan residues (Trp62 and Trp63) in the active site. As an adjacent pair of tryptophan residues can generate an extinction couple, this difference is interesting from a viewpoint of trytophan optical activity. Therefore, it is noteworthy that the spectrum shape of the Y63W human lysozyme, which has also an adjacent pair of tryptophan residues (Trp63 and Trp64), is not similar to that of the hen egg-white lysozyme but is similar to that of the wild-type human lysozyme. Since the shape of CD spectrum of either human lysozyme (Halper et al., 1971) or hen egg-white lysozyme (Glazer & Simmons, 1966) in this region is significantly affected by the changes in the environment of aromatic residues existing in the active cleft, it is suggested that the difference of CD spectra in this region between human lysozyme and hen egg-white lysozyme is not simply due to the difference between Trp and Tyr at this site, but should be attributed to the difference of another part of the molecule.

In Table III, the maximum wavelengths of fluorescence emission spectrum excited at 285 nm either in the absence or in the presence of 1 mM $(GlcNAc)_3$ are summarized. In contrast to the similarity of the maximum wavelengths of emission spectra among wild-type, Y63F mutant, and Y63L mutant human lysozyme in the absence of $(GlcNAc)_3$, the emission spectra of the Y63W and Y63A mutants were remarkably red-shifted as compared to wild-type human lysozyme and exhibited the same or longer maximum wavelengths than that of L-tryptophan. This indicates that a tryptophan residue exposed to solvent is present in the latter mutants. The fluorescence spectra of wild type, Y63W mutant human lysozyme, and hen egg-white lysozyme either in the absence or in the presence of 1 mM $(GlcNAc)_3$ are shown in Figure 5. In contrast to the similarity between the spectrum of wild-type human lysozyme and that of hen egg-white lysozyme, the spectrum of the Y63W human lysozyme is significantly different from that of either wild-type lysozyme. This suggests that the physicochemical environment of the introduced tryptophan residue in Y63W mutant is largely different from that of Trp62 in hen egg-white lysozyme. However, a similar blue shift was observed in the presence of $(GlcNAc)_3$ in every case (Figure 5), indicating that the environment of active-site tryptophans in the Y63W human lysozyme also became more hydrophobic due to the interaction with $(GlcNAc)_3$.

In general, the emission spectrum in protein excited at 285 nm is mainly derived from tryptophan residues, and the maximum wavelength of emission spectrum of tryptophan residue buried inside the molecule is considered to be blue-shifted as compared to that exposed to solvent (Teale, 1960). Thus, the accessible surface area of tryptophans probed with a water molecule of 1.4-Å radius was calculated (Lee & Richards, 1971) and summarized in Table IV. As expected from the structural similarity revealed by X-ray study, the

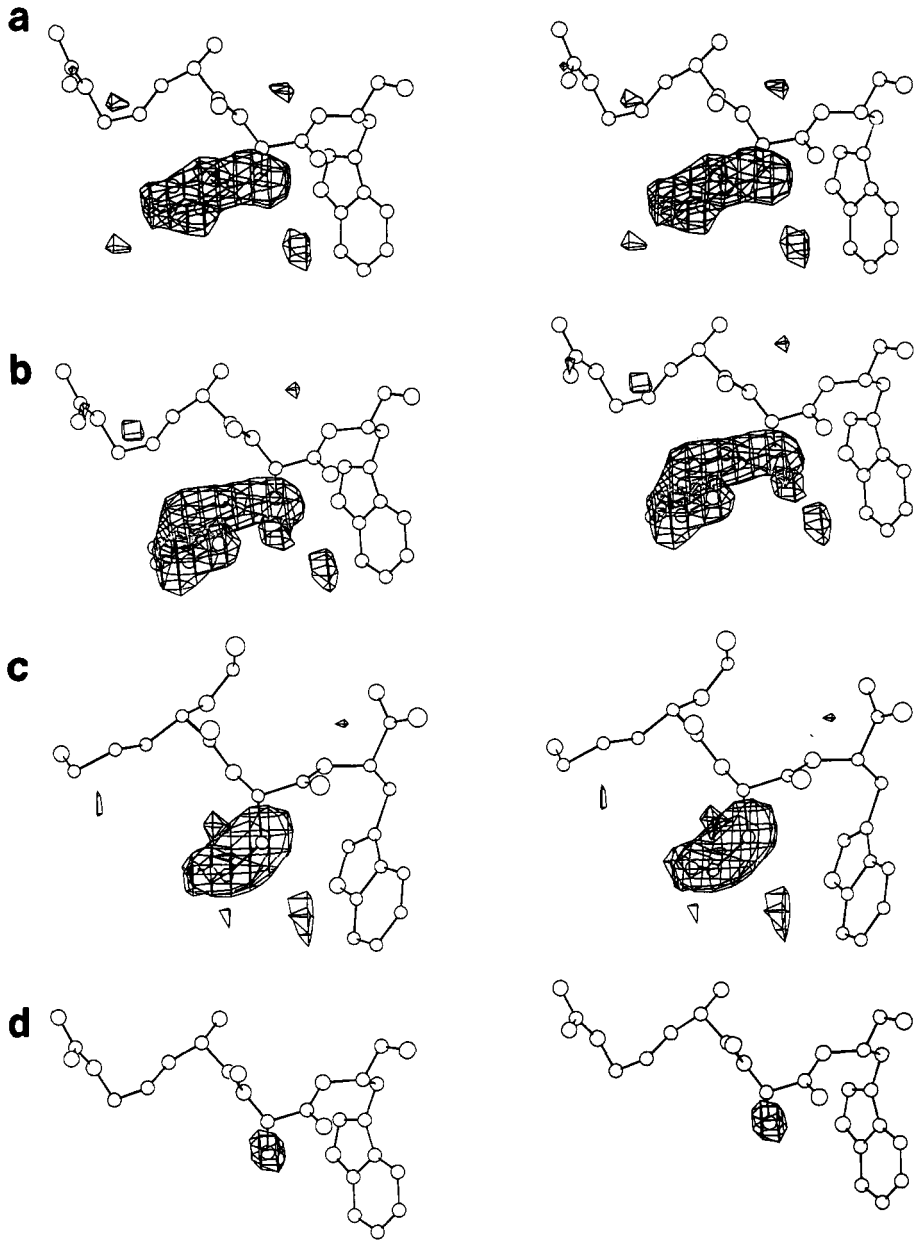

FIGURE 2: ($F_o - F_c$) maps showing the electron density of the side chains of 63rd residues. F_c and phases were calculated without the contribution of the side chain of the 63rd residue. (a) Y63F mutant; (b) Y63W mutant; (c) Y63L mutant; (d) Y63A mutant. Contour grids at the level of 0.2 eÅ^{-3} (for Y63F, Y63W, and Y63L mutants) or 0.3 eÅ^{-3} (for Y63A mutant) are shown.

largest difference was observed for the surface area of Trp64, the adjacent residue to the 63rd residue. The accessible surface area of Trp64 in the Y63A mutant was fairly large as compared to that of the Y63L mutant; however, it was almost the same as that of the Phe63 mutant or wild-type human lysozyme. The result suggests that the significant differences of maximum wavelength of emission spectra of the human lysozymes (Table III) cannot simply be attributed to the differences in the calculated surface area of the Trp64 residue probed with a water molecule, but rather to the differences in the hydrophobicity of the 63rd residue (Table IV), which can affect the actual accessibility of solvent molecules to the neighboring tryptophan residues, such as Trp64 and Trp109.

Function of Mutant Human Lysozymes. In Figure 6, the lysis curves of *M. luteus* cells caused by wild-type and mutant human lysozymes are shown. In contrast to the similarity of the curves of wild type, Y63F mutant, and Y63W mutant, the remaining mutants, especially the Y63L mutant, exhibited the lysis curve apparently constituted from the first rapidly decreasing period and the following more slowly decreasing period compared with that of wild-type enzyme. This behavior resembles that observed with the D53E mutant (Muraki et al., 1991). The effects of mutation on the inhibition of cell lysis by substrate analogs, $(GlcNAc)_3$ and $(GlcNAc)_2$, were investigated (Figure 7). These analogs inhibited the lytic activities of wild type, Y63F mutant, and Y63W mutant almost equally but inhibited those of the Y63L and Y63A mutants considerably less. In this connection, the dissociation constants (K_d) of $(GlcNAc)_3$ for mutant human lysozymes were examined in comparison with the wild-type enzyme by fluorometrical titrations. Wild type, Y63F mutant, and Y63W mutant showed the dissociation constants of similar level, and the order of affinity was wild type (K_d: 20 ± 7 μM) ≥ Y63F mutant (K_d: 29 ± 4 μM) > Y63W mutant (K_d: 55 ± 18 μM). The change in amplitude of emission spectrum of either Y63L or Y63A mutants when titrating with $(GlcNAc)_3$ was too small to determine the dissociation constant precisely. Even in the presence of 1 mM $(GlcNAc)_3$ the latter mutants indicated very small or almost negligible change in both the

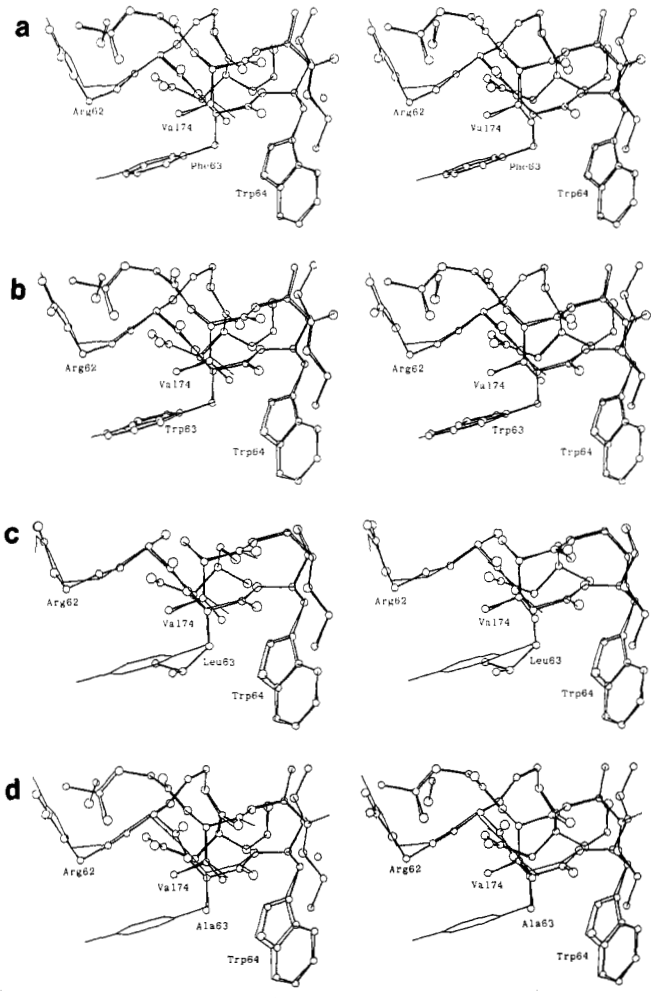

FIGURE 3: Local structures of mutant human lysozymes in the vicinity of the 63rd residue. (a) Y63F mutant; (b) Y63W mutant; (c) Y63L mutant; (d) Y63A mutant. The structure of the wild-type human lysozyme (Artymiuk & Blake, 1981) is superimposed and shown by thin lines.

shape and the intensity of emission spectra as compared to the spectra in the absence of $(GlcNAc)_3$.

Nanjo et al. (1988) indicated that PNP-$(GlcNAc)_5$ was cleaved by human lysozyme at the two major sites to produce PNP-GlcNAc and PNP-$(GlcNAc)_2$, respectively (Figure 8). In order to examine the effect of mutation at the 63th residue on the ratio of the productive binding modes, we investigated the cleavage patterns of PNP-$(GlcNAc)_5$ at the same two major sites of glycosidic bond as in the case of wild-type enzyme, however the ratio of the two major products somewhat changed depending on the kind of 63th residue (Table V). The percentages of all other cleavage products were less than 3% for wild-type and all mutant human lysozymes. Since Tyr63 in human lysozyme is considered to interact with the sugar residue that occupies subsite B, Tyr63 should be involved in both major productive binding modes (Figure 8).

The kinetic parameters concerning the decomposition of PNP-$(GlcNAc)_5$ were determined by measuring the initial rate of disappearance of PNP-$(GlcNAc)_5$ in the reaction mixture using HPLC with an area integrator. Due to both the solubility limit of PNP-$(GlcNAc)_5$ and the error magnitude in the measurement of peak area, the range of initial substrate concentration for the reliable measurement was restricted to ca. 3×10^{-4}–3×10^{-5} M. Within this range of initial concentration, the concentration of PNP-$(GlcNAc)_5$ decreased linearly up to about 80–85% of the initial concentration. The disappearance rate of PNP-$(GlcNAc)_5$ obeyed the Michaelis–Menten-type kinetics. In Table VI, the kinetic parameters concerning PNP-$(GlcNAc)_5$ disappearance obtained from the conventional double-reciprocal plot were shown. The Michaelis constant, K_M, for wild-type enzyme agrees well with the binding constant against $(GlcNAc)_5$ (48 μM) estimated from the fluorometric method (Teichberg et al., 1972). The maximum turn over number, k_{cat}, for wild-type enzyme is about one-tenth of that estimated for $(GlcNAc)_6$ (0.15 s^{-1}) with hen egg-white lysozyme (Benerjee et al., 1973), which is consistent with the ratio of the hydrolysis rate of $(GlcNAc)_6$ to that of $(GlcNAc)_5$ (Rupley & Gates, 1967). The conversion of Tyr63 to Phe or Trp did not largely affect both the K_M value and k_{cat} value, while the conversion of Tyr63 to Leu or Ala reduced the k_{cat}/K_M value to 2.2 ± 1.5% and 3.5 ± 3.1% of that of the wild-type enzyme, respectively. Analysis of kinetic parameters indicated that the substantial change in enzymatic activity caused by the latter mutations should mainly be attributed to the change in affinity between the enzyme and the substrate. The difference in binding energy of the enzyme with the substrate in the transition state, ΔG_R, was estimated from the ratio of k_{cat}/K_M for each mutant to wild-type enzyme as described by Wilkinson et al. (1983) (Table VI). The comparison of ΔG_R value between wild-type and Y63F mutant and that between wild-type and Y63A mutant indicated that the apparent contributions of the phenolic hydroxyl group and that of the phenol group in the side chain of Tyr63 amount to 0.4 ± 0.4 and 2.5 ± 0.8 kcal mol^{-1}, respectively.

DISCUSSION

van der Waals contacts as well as hydrogen bonding interactions are extensively utilized in the recognition of carbohydrate molecules by proteins (Quiocho, 1986). Until now, several examples that an aromatic residue makes either partial stacking or face-to-face contact with a sugar residue were identified by X-ray crystallographic studies on protein–carbohydrate ligand complexes. The aromatic residues in such complexes include Trp340 of maltose binding protein (Spurlino et al., 1991), Trp135, Trp269, and Trp367 in *Trichoderma reesei* cellulase (Rouvinen et al., 1990) and Trp62 of hen egg-white lysozyme (Blake et al., 1967). This suggests that the van der Waals contacts employing the side chain of aromatic residues are ubiquitiously engaged in the interactions crucial to the carbohydrate ligand binding. However, the extent of the functional contributions of each structural element of a particular residue in either the overall stability of protein–sugar complexes or the overall catalytic activities of sugar-recognizing enzymes is difficult to ascertain, unless the characterization of either the suitable mutant proteins or the sugar ligands specifically modified at the interaction site in question is performed in terms of both the functional changes and the structural consequences caused by the modifications. Tyr63 of human lysozyme structurally corresponds to Trp62 of hen egg-white lysozyme, and this residue is also considered to be involved in van der Waals interaction with sugar residues that occupy subsite B based on the results of the X-ray crystallographic analysis of the complex with either $(GlcNAc)_3$ (Matsushima et al., 1990) and $(GlcNAc)_5$ (Inaka et al., 1990).

Site-directed mutagenesis is ideal for dissecting each contribution of structural elements of a tyrosine residue in the recognition of ligand. The contribution of phenolic hydroxyl group, which may serve as a donor or an acceptor of the hydrogen bond with substrate, can be assessed by the conversion to Phe, the contribution of the phenol group by the conversion to Ala, and the contribution of planarity of the

Table II: Comparison of Structures between Wild-Type and Mutant Human Lysozymes

rms difference[a] in	Y63F	Y63W	Y63L	Y63A
main chain atoms (Å)	0.122	0.125	0.146	0.135
side-chain atoms of major residues composing active site[b] (Å)	0.128	0.110	0.148	0.137
side-chain atoms of catalytic residues[c] (Å)	0.077	0.075	0.106	0.072

[a] Root mean square difference. [b] Side-chain atoms of Glu35, Asp53, Trp64, Asp102, and Trp109. [c] Side-chain atoms of Glu35 and Asp53.

Table III: Maximum Wavelength of Fluorescence Emission Spectrum[a]

	wild type	Y63F	Y63W	Y36L	Y63A	hen[b]	L-tryptophan
in absence of $(GlcNAc)_3$	334	337	359	339	362	342	359
in presence of $(GlcNAc)_3$[c]	330	328	357	337	362	329	ND[d]

[a] Not corrected: excitation wavelength, 285 nm; protein concentration, 3.0 μM. [b] Hen egg-white lysozyme. [c] Concentration of $(GlcNAc)_3$, 1 mM. [d] Not determined.

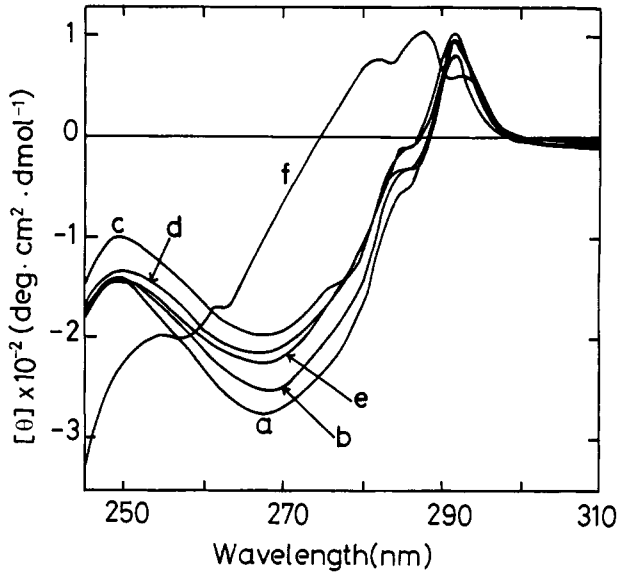

FIGURE 4: Comparison of CD spectra. (a) Wild-type human lysozyme; (b) Y63F mutant; (c) Y63W mutant; (d) Y63L mutant; (e) Y63A mutant; (f) hen egg-white lysozyme. Protein concentration: 0.33 mg/mL in 25 mM sodium phosphate buffer (pH 8.0) plus 0.27 M NaCl.

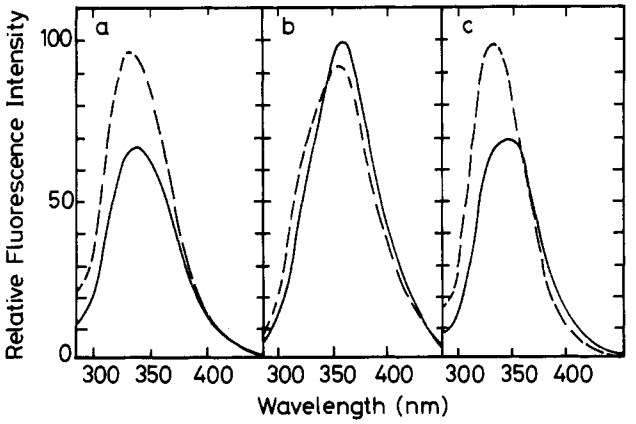

FIGURE 5: Fluorescence spectra in the absence (—) or the presence (– –) of $(GlcNAc)_3$ (1 mM). (a) Wild-type human lysozyme; (b) Y63W human lysozyme; (c) hen egg-white human lysozyme. Protein concentration: 3 μM in McIlvaine buffer (pH 7.2), excited at 285 nm, not corrected.

Table IV: Solvent-Accessible Surface Area[a] of Tryptophan Residues and Hydrophobicity Scale[b] of 63rd Residue

	wild type	Y63F	Y63W	Y63L	Y63A
solvent-accessible area (Å²) of					
Trp28	0.0	0.0	0.0	0.0	0.0
Trp34	104.8	101.3	102.3	101.9	105.7
Trp64	26.0	24.1	22.8	19.0	26.1
Trp109	18.4	18.5	19.3	16.9	16.9
Trp112	15.2	15.0	14.8	18.2	15.2
hydrophobicity scale of 63rd residue (kcal mol⁻¹)	2.3	2.5	3.4	1.8	0.5

[a] Probe radius, 1.4 Å. [b] From Nozaki and Tanford (1971).

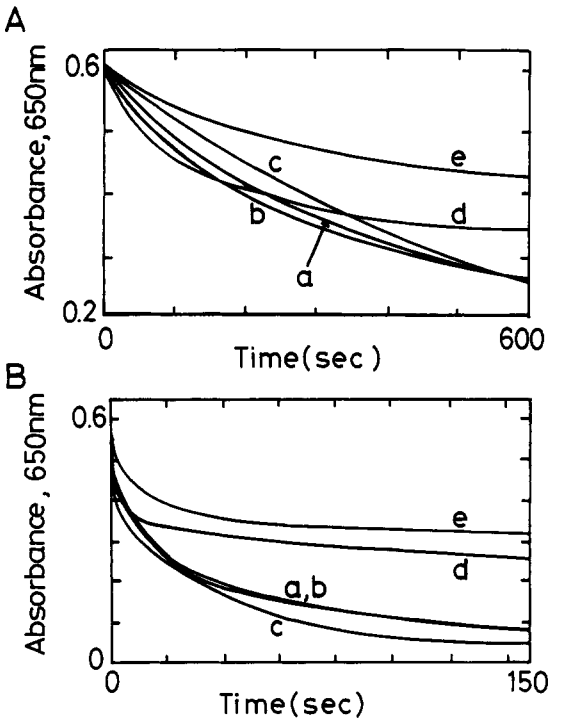

FIGURE 6: Lysis of *M. luteus* cells by wild-type and mutant human lysozyme. (a) Wild type; (b) Y63F mutant; (c) Y63W mutant; (d) Y63L mutant; (e) Y63A mutant. Enzyme concentration, (A) 0.25 μg/mL; (B) 4.0 μg/mL and substrate concentration, 0.25 mg/mL in 50 mM potassium phosphate buffer (pH 6.2). Measurements were performed at 25 °C.

side chain by the conversion to Leu, which has the side chain of nonplanar but similar hydrophobicity to Tyr (Nozaki & Tanford, 1971). X-ray crystallographic analysis revealed that no remarkable change has occurred in the active-site conformation, including the position of catalytic residues except the mutation point in any mutants in the present study (Figure 3 and Table II). In spite of the effect of mutations on the lysis curve of bacterial substrate, which indicates the large decrease in the lysis rate at the early stage of reaction, the hydrolysis of PNP-$(GlcNAc)_5$ by the Y63L and Y63A mutants proceeded linearly at the early stage of reaction in contrast to the D53E mutant which did not show the constant activity even at the early stage of the reaction (Muraki et al., 1991). Since a lysis curve is obtained by measuring the decrease of the turbidity

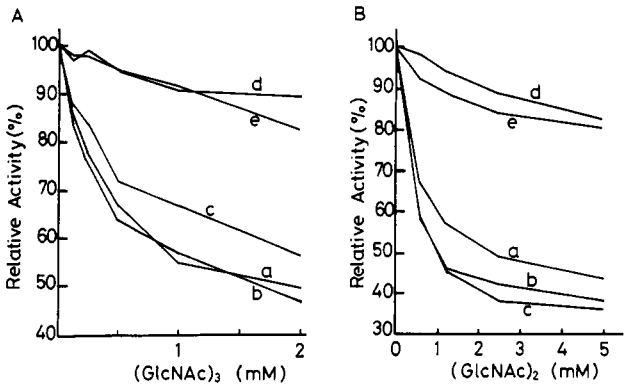

FIGURE 7: Inhibition of cell lysis by $(GlcNAc)_3$ and $(GlcNAc)_2$. (a) Wild-type human lysozyme; (b) Y63F mutant; (c) Y63W mutant; (d) Y63L mutant; (e) Y63A mutant. Enzyme concentration, 0.3 μg/mL and substrate concentration, 0.25 mg/mL in 50 mM potassium phosphate. Reaction was performed at 30 °C for 2 min in the presence of several concentrations of $(GlcNAc)_3$ (A) or $(GlcNAc)_2$ (B). Relative activity was calculated from the change in the absorbance at 650 nm.

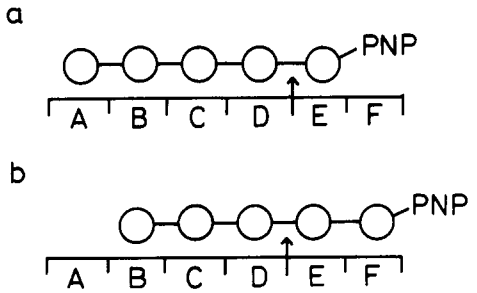

FIGURE 8: Major productive binding modes of PNP-$(GlcNAc)_5$ to the subsites of human lysozyme. O, GlcNAc residue; PNP, *p*-nitrophenol group. A–F indicate the subsites of human lysozyme. Tyr63 locates at subsite B. The glycosidic bond between the GlcNAc residues that occupy subsite D and subsite E (indicated by an arrow) is cleaved to produce PNP-GlcNAc plus $(GlcNAc)_4$ (mode a) and PNP-$(GlcNAc)_2$ plus $(GlcNAc)_3$ (mode b), respectively.

Table V: Production Ratio[a] of PNP-GlcNAc to PNP-$(GlcNAc)_2$ in Cleavage of PNP-$(GlcNAc)_5$ by Wild-Type and Mutant Human Lysozymes[b]

	wild type	Y63F	Y63W	Y63L	Y63A
production ratio of PNP-GlcNAc to PNP-$(GlcNAc)_2$	3.1	2.8	2.2	1.5	1.0

[a] PNP-GlcNAc/PNP-$(GlcNAc)_2$. [b] Initial concentration of PNP-$(GlcNAc)_5$: 2.3×10^{-4} M, at 37 °C in 100 mM sodium citrate buffer (pH 5.0). Enzyme concentration, 20 μg/mL (wild type, Y36F mutant, Y63W mutant), 90 μg/mL (Y63L and Y63A mutants).

Table VI: Kinetic Parameters of Wild-Type and Mutant Human Lysozymes for PNP-$(GlcNAc)_5$[a]

enzyme	K_M (μM)	k_{cat} (s^{-1})	k_{cat}/K_M (M^{-1} s^{-1})	ΔG_R[b] (kcal mol^{-1})
wild type	54 ± 9	0.013 ± 0.002	250 ± 80	
Y63F	79 ± 12	0.010 ± 0.001	130 ± 30	0.4 ± 0.4
Y63W	86 ± 15	0.0058 ± 0.0003	70 ± 16	0.8 ± 0.3
Y63L	1600 ± 500	0.0058 ± 0.0010	4.3 ± 2.0	2.6 ± 0.6
Y63A	960 ± 480	0.0038 ± 0.0016	6.4 ± 4.9	2.5 ± 0.8

[a] Obtained from the initial rate of disappearance of PNP-$(GlcNAc)_5$. [b] $\Delta G_R = -RT \ln [(k_{cat}/K_M)_{mutant}/(k_{cat}/K_M)_{wild\ type}]$; calculated at 37 °C; *R*, gas constant.

of a reaction mixture, it does not always correspond to the net hydrolytic activity. Therefore, the effect of mutation on the lysis curve observed in the Y63L and Y63A mutants may indicate that these mutants prefer the smaller fragments of the bacterial cell wall which contribute less to the turbidity of reaction mixture than the larger ones in their substrate compared with the wild-type enzyme.

In all aspects of the enzymatic characterization, the Y63F and Y63W mutants, which have planar side chains at the 63rd residue, exhibited behavior similar to the wild-type enzyme, while the Y63L and Y63A mutants were characterized as the mutants that have lost the affinity toward $(GlcNAc)_2$, $(GlcNAc)_3$, or PNP-$(GlcNAc)_5$ significantly. The result in the present study rules out the possibility of involvement of either the hydrogen bonding via the phenolic hydroxyl group of Tyr63 or the hydrophobic properties themself as a major determinant of specificity toward the electrostatically neutral substrates as PNP-$(GlcNAc)_5$ in the catalytic reaction of human lysozyme. On the other hand, the kinetic analysis indicated that deletion of the phenol group from Tyr63 using the conversion of Tyr63 to Ala weakened the binding energy in the transition state for the hydrolysis of PNP-$(GlcNAc)_5$ by 2.5 ± 0.8 kcal mol^{-1}. This value of energy difference roughly corresponds to either the energy change in the double of the deletion of a side chain on the enzyme that forms a good hydrogen bond with an uncharged group on the substrate or that in the deletion of an uncharged side chain on the enzyme that forms a hydrogen bond with a charged group on the substrate (Fersht et al., 1985). The binding and kinetic data revealed that the decrease of catalytic activity due to the replacement of Tyr63 to either Leu or Ala ought to be mainly attributed to the reduction of affinity between enzyme and substrate. The increase of apparent K_m value in Y63L or Y63A mutants may arise not only from the decrease of van der Waals contacts between the side chain of the 63rd residue and the sugar residue at subsite B in the productive binding mode but also from the relative increase of nonproductive binding, including the occurrence of novel binding conformation of substrate in the active site. More detailed mechanism of the increase of K_m value should be discussed on the basis of both the structure of Y63L or Y63A mutants in the presence of a substrate analog and the results of further kinetic analysis, but the X-ray structures and the kinetic data in the present study strongly suggest that the direct contact between the planar side-chain group of Tyr63 and the sugar residue at subsite B is substantially involved in the catalytic action of human lysozyme toward a electrostatically neutral substrate. Another example of the decrease of catalytic activity caused by the loss of planarity of the side-chain group of an aromatic residue, Trp62, was reported on hen egg-white lysozyme (Blake et al., 1981). This together with our result suggests that it may be possible to increase the binding strength toward a carbohydrate ligand by some dozen times, if an aromatic residue is properly introduced into the potential carbohydrate binding site without bringing in an unnecessary steric hindrance.

Our present study also indicated that in spite of the apparent close similarity in the active site structure between human lysozyme and hen egg-white lysozyme (Artymiuk & Blake, 1981), the physicochemical circumstance of Trp63 in the Y63W human lysozyme is not always the same as that of Trp62 in hen egg-white lysozyme and that the affinity of the Y63W human lysozyme toward $(GlcNAc)_3$ is somewhat weaker than either that of wild-type human lysozyme (Teichberg et al., 1972) or that of hen egg-white lysozyme (Chipman et al., 1967). This suggests that not only the presence of an aromatic residue but also the precise positioning and the surrounding physicochemical circumstance are critical

for the expression of the optimum affinity toward carbohydrate moiety.

REFERENCES

Artymiuk, P. J., & Blake, C. C. F. (1981) *J. Mol. Biol. 152*, 737–762.

Banerjee, S. K., Kregar, I., Turk, V., & Rupley, J. A. (1973) *J. Biol. Chem. 248*, 4786–4792.

Blake, C. C. F., Johnson, L. N., Mair, G. A., North, A. C. T., Phillips, D. C., & Sarma, V. R. (1967) *Proc. R. Soc. London Ser. B167*, 378–388.

Blake, C. C. F., Cassels, R., Dobson, C. M., Poulsen, F. M., Williams, R. J. P., & Wilson, K. S. (1981) *J. Mol. Biol. 147*, 73–95.

Brünger, A. T., Kuriyan, J., & Karplus, M. (1987) *Science 35*, 458–460.

Chipman, D. M., Grisaro, V., & Sharon, N. (1967) *J. Biol. Chem. 242*, 4388–4394.

Fersht, A. R., Shi, J.-P., Knill-Jones, J., Lowe, D. M., Wilkinson, A. J., Blow, D. M., Brick, P., Carter, P., Waye, M. M. Y., & Winter, G. (1985) *Nature 314*, 235–238.

Glazer, A. N., & Simmons, N. S. (1966) *J. Am. Chem. Soc. 88*, 2335–2336.

Halper, J. P., Latovitzki, N., Bernstein, H., & Beychok, S. (1971) *Proc. Natl. Acad. Sci. U.S.A. 68*, 517–522.

Hayashi, K., Imoto, T., Funatsu, G., & Funatsu, M. (1965) *J. Biochem. (Tokyo) 58*, 227–235.

Imoto, T., Johnson, L. N., North, A. C. T., Phillips, D. C., & Rupley, J. A. (1972) in *The Enzymes* (Boyer, P. D., Ed.) Vol. 7, Chapter 21, Academic Press, New York.

Imoto, T., Fujimoto, M., & Yagishita, K. (1974) *J. Biochem. (Tokyo) 76*, 745–753.

Inaka, K., Matsushima, M., & Morikawa, K. (1990) *Acta Crystallogr. A46*, C85.

Jigami, Y., Muraki, M., Harada, N., & Tanaka, H. (1986) *Gene 43*, 273–279.

Kumagai, I., & Miura, K. (1989) *J. Biochem. (Tokyo) 105*, 946–948.

Kuroda, M., Sakiyama, F., & Narita, K. (1975) *J. Biochem. (Tokyo) 78*, 641–651.

Lee, B., & Richards, F. M. (1971) *J. Mol. Biol. 55*, 379–400.

Locquet, J. P., Saint-Blancard, J., & Jollès, P. (1968) *Biochim. Biophys. Acta 167*, 150–153.

Luzzati, V. (1952) *Acta Crystallogr. 5*, 802–810.

Matsushima, M., Inaka, K., & Morikawa, K. (1990) *Acta Crystallogr. A46*, C82.

McIlvaine, T. C. (1921) *J. Biol. Chem. 49*, 183–186.

Muraki, M., Morikawa, M., Jigami, Y., & Tanaka, H. (1987) *Biochim. Biophys. Acta 916*, 66–75.

Muraki, M., Morikawa, M., Jigami, Y., & Tanaka, H. (1989) *Eur. J. Biochem. 179*, 573–579.

Muraki, M., Harata, K., Hayashi, Y., Machida, M., & Jigami, Y. (1991) *Biochim. Biophys. Acta 1079*, 229–237.

Nanjo, F., Sakai, K., & Usui, T. (1988) *J. Biochem. (Tokyo) 104*, 255–258.

Nozaki, Y., & Tanford, C. (1971) *J. Biol. Chem. 246*, 2211–2217.

Ohkubo, T., Taniyama, Y., & Kikuchi, M. (1991) *J. Biochem. (Tokyo) 110*, 1022–1029.

Osserman, E. F., Cole, S. J., Swan, I. D. A., & Blake, C. C. F. (1969) *J. Mol. Biol. 46*, 211–212.

Osserman, E. F., Canfield, R. E., & Beychok, S., Ed. (1972) *Lysozyme*, Academic Press, New York.

Parry, R. M., Jr., Chandan, R. C., & Shahani, K. M. (1969) *Arch. Biochem. Biophys. 103*, 59–65.

Phillips, D. C., Acharya, K. R., Handoll, H. M. G., & Stuart, D. I. (1987) *Biochem. Soc. Trans. 15*, 737–744.

Quiocho, F. A. (1986) *Annu. Rev. Biochem. 55*, 287–315.

Redfield, C., & Dobson, C. M. (1990) *Biochemistry 29*, 7201–7214.

Rouvinen, J., Bergfors, T., Teeri, T., Knowles, J. K. C., & Jones, T. A. (1990) *Science 249*, 380–386.

Rupley, J. A., & Gates, V. (1967) *Proc. Natl. Acad. Sci. U.S.A. 57*, 496–510.

Shrake, A., & Rupley, J. A. (1980) *Biochemistry 19*, 4044–4051.

Spurlino, J. C., Lu, G.-Y., & Quiocho, F. A. (1991) *J. Biol. Chem. 266*, 5202–5219.

Teale, F. W. J. (1960) *Biochem. J. 76*, 381–388.

Teichberg, V. I., Plasse, T., Sorell, S., & Sharon, N. (1972) *Biochim. Biophys. Acta 278*, 250–257.

Thaller, C., Eichele, G., Weaver, J. H., Wilson, E., Karlsson, R., & Jansonius, J. N. (1985) *Methods Enzymol. 114*, 132–135.

Wilkinson, A. J., Fersht, A. R., Blow, D. M., & Winter, G. (1983) *Biochemistry 22*, 3581–3586.

Yamasaki, N., Tsujita, T., Sakiyama, F., & Narita, K. (1976) *J. Biochem. (Tokyo) 80*, 409–412.